

Isoscalar $E0$, $E1$, and $E2$ strength in ^{40}Ca

D. H. Youngblood, Y.-W. Lui, and H. L. Clark
 Cyclotron Institute, Texas A&M University, College Station, Texas 77840
 (Received 12 February 2001; published 3 May 2001)

The giant resonance region from $10 < E_x < 55$ MeV in ^{40}Ca has been studied with inelastic scattering of 240-MeV α particles at small angles including 0° . Strength corresponding to $97 \pm 11\%$, $108 \pm 12\%$, and $62 \pm 10\text{--}20\%$ of the isoscalar $E0$, $E2$, and $E1$ sum rules, respectively, was identified with centroids of 19.18 ± 0.37 MeV, 17.84 ± 0.43 MeV, 23.36 ± 0.70 MeV, and rms widths of 4.88 ± 0.57 MeV, 2.89 ± 0.60 MeV, and 5.34 ± 0.90 MeV.

DOI: 10.1103/PhysRevC.63.067301

PACS number(s): 25.55.Ci, 24.30.Cz, 27.40.+z

The location of the isoscalar giant monopole resonance is important because its energy can be directly related to the nuclear compressibility and from this the compressibility of nuclear matter (K_{NM}) can be obtained. In a previous report [1] evidence was presented for the location of $92 \pm 15\%$ of the $E0$ sum rule in ^{40}Ca , but a definitive assignment could be made only for $33 \pm 4\%$ of the $E0$ strength. The location of this strength is consistent with $K_{\text{NM}} = 231 \pm 4$ MeV obtained from giant monopole resonance energies of four heavier nuclei [2]. In Ref. [1] the spectrum subtraction technique was used to highlight $E0$ strength, however, this technique is particularly sensitive to experimental background, detector response functions, and the presence of other multipolarities. We report here new data for Ca over the range $10 < E_x < 55$ MeV (the data in Ref. [1] covered $4 < E_x < 27$ MeV) and use an analysis technique which unambiguously identifies multipole strength [3] even when it is distributed over a large excitation range.

The experimental technique has been described thoroughly in Ref. [3] and is summarized briefly below. A beam of 240-MeV α particles from the Texas A&M K500 superconducting cyclotron bombarded a self-supporting natural Ca foil 2.0 mg/cm^2 thick located in the target chamber of the multipole-dipole-multipole spectrometer. The horizontal acceptance of the spectrometer was 4° and ray tracing was used to reconstruct the scattering angle. The vertical acceptance was set at $\pm 2^\circ$. The focal plane detector covered from 47 to 55 MeV of excitation, depending on scattering angle, and measured position and angle in the scattering plane. The out-of-plane scattering angle was not measured. Position resolution of approximately 0.9 mm and scattering angle resolution of about 0.09° were obtained. Cross sections were obtained from the charge collected, target thickness, dead time, and known solid angle. The cumulative uncertainties in target thickness, solid angle, etc., result in about a $\pm 10\%$ uncertainty in absolute cross sections.

Sample spectra obtained are shown in Fig. 1. The giant resonance peak can be seen extending up past $E_x = 35$ MeV. The spectrum was divided into a peak and a continuum where the continuum was assumed to have the shape of a straight line at high excitation joining onto a Fermi shape at low excitation [Eq. (1)] to model particle threshold effects,

$$Y(\text{continuum}) = A + B * E_x + Y_0^* [1 + \exp(E_x - E_{\text{th}})/C]. \quad (1)$$

A and B are determined from a fit to the high excitation region ($E_x = 42\text{--}52$ MeV), E_{th} and C are adjusted to model the behavior of the spectrum near the particle threshold, and Y_0 is adjusted so that the continuum obtained is zero in the region just below the particle threshold ($E_x = 6\text{--}7$ MeV). The parameters E_{th} and C were fixed to be the same for all spectra, while A , B , and Y_0 were required to change continuously as a function of angle for all spectra taken at the same spectrometer angle (a ‘‘data set’’). The continua used are shown by the dashed lines in Fig. 1.

The multipole components of the giant resonance peak were obtained [3] by dividing the peak into multiple regions (bins) by excitation energy and then comparing the angular distributions obtained for each of these bins to distorted-wave Born-approximation (DWBA) calculations to obtain the multipole components. The uncertainty from the multipole fits was determined for each multipole by incrementing (or decrementing) that strength, then adjusting the strengths of the other multipoles to minimize total χ^2 . This continued until the new χ^2 was one unit larger than the total χ^2 obtained for the best fit.

The DWBA calculations were described in Ref. [1] and the same Gaussian Woods-Saxon folding potentials were used for the calculations in this work. A sample of the angular distributions obtained for the giant resonance (GR) peak and the continuum are shown in Fig. 2. Fits to the angular distributions were carried out with a sum of isoscalar 0^+ , 1^- , 2^+ , 3^- , and 4^+ strengths. The isovector giant dipole resonance (IVGDR) contributions are small, but were calculated from the known distribution [4] and held fixed in the fits. Sample fits obtained, along with the individual components of the fits, are shown superimposed on the data in Fig. 2.

The (isoscalar) $E0$, $E1$, and $E2$ multipole distributions obtained are shown in Fig. 3 and the results are summarized in Table I. Due to the limited angular range of the data, $E3$ and $E4$ strength could not be distinguished unambiguously. Several analyses were carried out to assess the effects of different choices of the continuum as well as the effects of different bin sizes on the resulting multipole distributions. In the ^{24}Mg analysis [3] it was demonstrated that $E0$ strength in the peak and continuum could be identified, and that the total $E0$ strength obtained does not depend strongly on the continuum choice. However, in the ^{24}Mg analysis [3] it was also demonstrated that other processes in the continuum gave an-

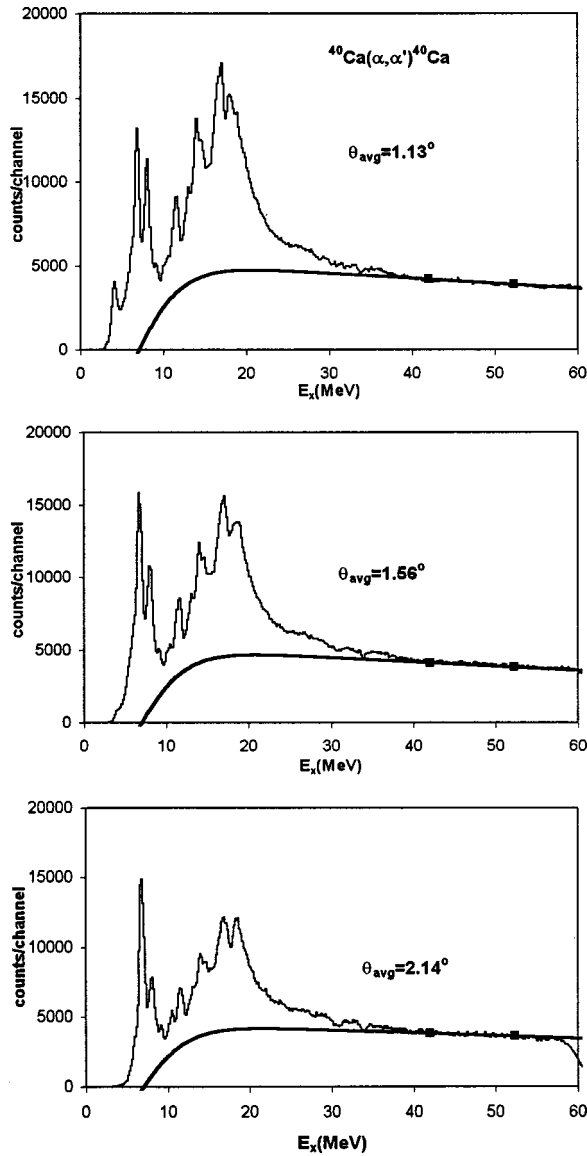


FIG. 1. Inelastic α spectra obtained with the spectrometer at 0° . The thick lines show the continuum chosen for the analysis. The black squares indicate the region fit to determine the linear parameters (see text).

gular distributions that could be fit with a sum of $E1$, $E2$, $E3$, and $E4$ multipole strengths and hence strength distributions for these multipoles could be sensitive to assumptions about the continuum. Therefore the effects of several different continuum choices were explored. Analyses were made using continua chosen with several different criteria [e.g., (a) using slightly incorrect slopes on the linear part with the continuum shape from Eq. (1), (b) using the method of Ref. [3] where the entire continuum is represented by a polynomial independently for each angle, and (c) deliberately altering the continuum slope and/or amplitude at only selected angles]. These had only small effects on the $E0$ parameters with m_1/m_0 varying at most ± 250 keV from the value in Table I, and the sum-rule strength varying from 94–104 % of the $E0$ energy weighted sum rule (EWSR). This stability is likely due to the strongly forward peaked nature of the $E0$

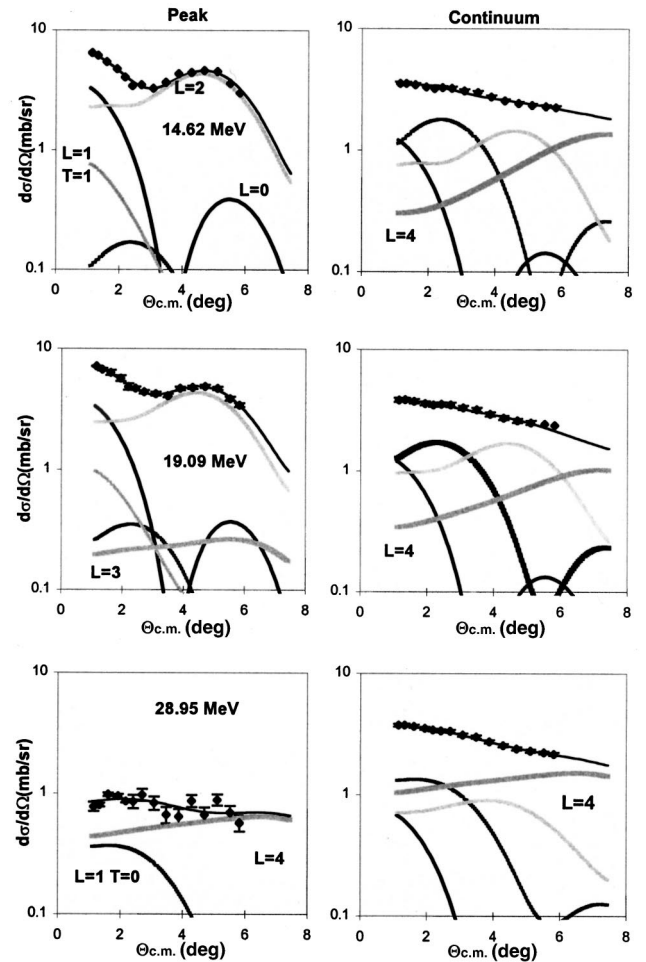


FIG. 2. Angular distributions obtained for inelastic α scattering for three excitation ranges of the GR peak and the continuum in ^{40}Ca . Thin lines show the fits. Contributions of each multipole are shown. When not shown, errors are smaller than the data points.

strength, which allows us to extract $E0$ strength from the continuum. The $E2$ strength in the peak was also reasonably stable, with m_1/m_0 varying ± 400 keV and the sum-rule strength varying from 102–120 %. This is probably due in large part to the excellent peak/continuum ratio. The extracted isoscalar $E1$ strength distribution was much more sensitive to the continuum choice, however, with m_1/m_0 shifts up to 2.5 MeV and sum-rule variation from 28–94 % of the $E1$ EWSR. The extreme values were from continuum choices that appeared nonphysical, but these same extreme choices had much smaller effects on the $E0$ and $E2$ distributions. There are at least two major contributors to this sensitivity of the $E1$ strength. The $E1$ cross section to continuum ratio is fairly small. Also the $E1$ angular distribution peaks in the valley of the $E0$ distribution, making the extracted $E1$ strength strongly dependent on the peak/valley ratio of the angular distribution, which is particularly sensitive to continuum choices.

The $E0$ distribution obtained from spectrum subtraction [1] is shown superimposed in Fig. 3 and is generally in agreement with the multipole analysis. The strength below $E_x = 10$ MeV could not be extracted in the present experi-

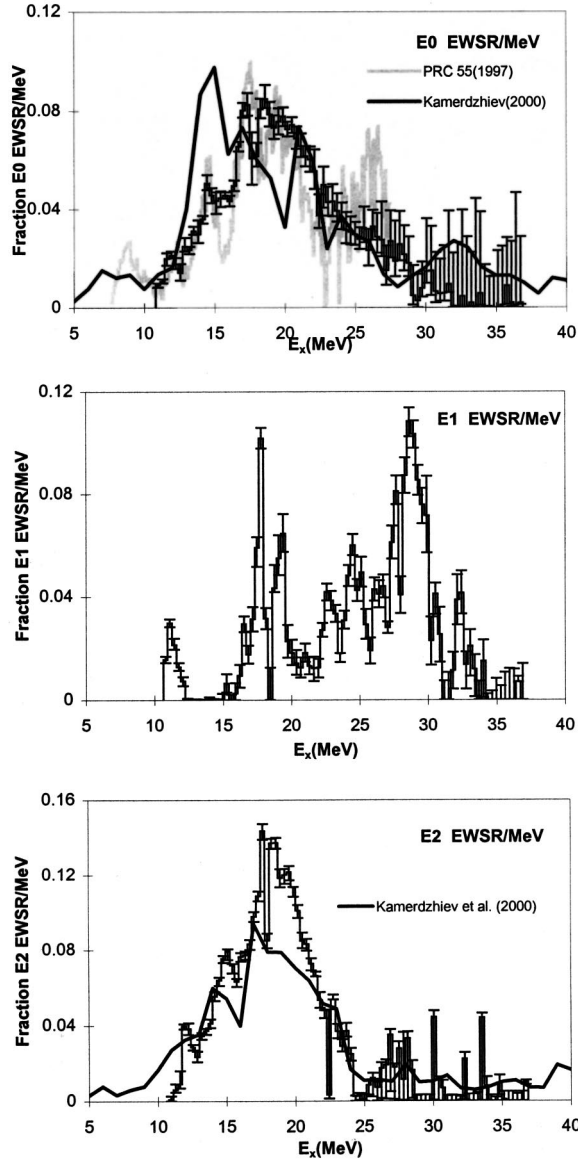


FIG. 3. Strength distributions obtained are shown by the histograms. Error bars represent the uncertainty due to the fitting of the angular distributions as described in the text. The thick black line shows calculations by Kamezdzhiev *et al.* [12] while the gray line shows the $E0$ distribution reported in Ref. [1].

ment. The peak at the upper excitation edge of the detector in the earlier experiment (around $E_x = 25$ MeV) is absent in the multipole analysis, and $E0$ strength is seen in the present experiment well above the upper energy limit of Ref. [1]. If we include the strength below $E_x = 10$ MeV from the previ-

TABLE I. Multipole parameters obtained for ^{40}Ca .

	m_1/m_0 (MeV)	rms width (MeV)	% EWSR
$E0$	19.18 ± 0.37	4.88 ± 0.57	97 ± 11
$E2$	17.84 ± 0.43	2.89 ± 0.60	108 ± 12
$E1 (T=0)$	23.36 ± 0.70	5.34 ± 0.90	$62 + 10 - 20$

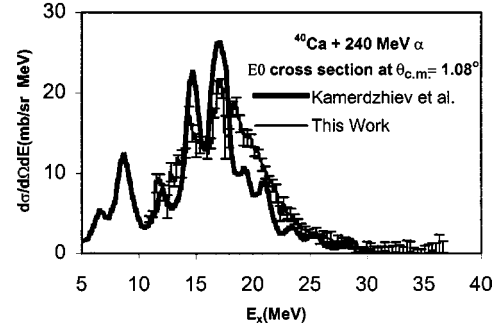


FIG. 4. The $E0$ cross section for α scattering at $\theta_{c.m.} = 1.08^\circ$ is shown by the histogram. That calculated by Kamezdzhiev *et al.* [12] is shown by the wide black line. The error bars represent the uncertainty in obtaining the $E0$ strength distribution.

ous experiment (not definitively assigned to $E0$), then m_1/m_0 becomes 18.70 ± 0.42 MeV, $(m_1/m_{-1})^{1/2} = 17.22 \pm 0.41$ MeV, $(m_3/m_1)^{1/2} = 20.76 \pm 0.51$ MeV and $112 \pm 13\%$ of the $E0$ EWSR would be accounted for. Comparing $(m_1/m_{-1})^{1/2}$ to the calculations of Blaizot *et al.* [2,5] results in a K_{nm} of 236 ± 6 MeV, in agreement with the conclusions in Ref. [1].

The $E2$ strength observed corresponds to $108 \pm 12\%$ of the $E2$ EWSR with a centroid of 17.84 MeV. Previous studies [1,6,7] identified approximately half of the EWSR strength centered around 17.8 MeV, with the exception of a (π, π') study [8] that reported 77% of the $E2$ EWSR centered at $E_x = 18.2$ MeV. The present results differ from those reported in Ref. [1] primarily because with the much larger excitation energy range of the present data it is clear that the continuum is considerably lower than thought previously, resulting in considerably more $E2$ strength in the peak.

Isoscalar $E1$ strength corresponding to $62 + 10 - 20\%$ of the $E1$ EWSR was identified with a centroid of 23.36 ± 0.70 MeV and an rms width of 5.34 MeV. Below $E_x = 10$ MeV, $4.25 \pm 0.27\%$ of the $E1$ EWSR is known [9], bringing the total reported to 66% of the isoscalar $E1$ EWSR. Previously Rost *et al.* [10] had concluded that isoscalar $E1$ strength was required at approximately $E_x = 14.3$ and 16 MeV in ^{40}Ca to fit (α, α') angular distributions taken at $E_\alpha = 104$ MeV, however, the cross sections required to fit their data correspond to approximately 49% and 28% of the $E1$ EWSR for the two regions when calculated with optical parameters from Ref. [6] and the form factor as described by Harakeh and Dieperink [11]. This far exceeds the strength we obtain in that region.

Kamezdzhiev *et al.* [12] have carried out microscopic calculations in continuum random-phase approximation (RPA) including $1p1h$ coupled to phonon configurations for both ^{58}Ni and ^{40}Ca . For ^{58}Ni they calculate expected cross sections as a function of E_x for a 240-MeV inelastic α particle scattering including $L=0-4$ and get excellent agreement with our ^{58}Ni results [13]. For ^{40}Ca they report isoscalar $E0$ and $E2$ strength distributions as well as a cross section for $E0$ strength for 240-MeV inelastic α particle scattering at 1.08° . Superimposed in Fig. 3 are their $E0$ and $E2$ strength distributions. Both are in fairly good agreement with our measured distributions, though their predicted $E2$ strength is

distributed more broadly than the experimental result. Their microscopic $E0$ transition densities change significantly over the excitation range, so that a direct comparison of their strength distribution with the one we extract with a constant transition density could be misleading. Therefore we have used the strength distribution shown in Fig. 3 and calculated

an equivalent $1.08^\circ E0$ cross section and that is compared to their calculation in Fig. 4. The agreement is quite remarkable.

This work was supported in part by the U.S. Department of Energy under Grant No. DE-FG03-93ER40773 and by The Robert A. Welch Foundation.

-
- [1] D. H. Youngblood, Y.-W. Lui, and H. L. Clark, Phys. Rev. C **55**, 2811 (1997).
 - [2] D. H. Youngblood, H. L. Clark, and Y.-W. Lui, Phys. Rev. Lett. **82**, 691 (1999).
 - [3] D. H. Youngblood, Y.-W. Lui, and H. L. Clark, Phys. Rev. C **60**, 014304 (1999).
 - [4] S. S. Dietrich and B. L. Berman, At. Data Nucl. Data Tables **38**, 199 (1988).
 - [5] J. P. Blaizot *et al.*, Nucl. Phys. **A591**, 435 (1995).
 - [6] Y.-W. Lui, J. D. Bronson, C. M. Rozsa, D. H. Youngblood, P. Bogucki, and U. Garg, Phys. Rev. C **24**, 884 (1981).
 - [7] S. Brandenburg, R. de Leo, A. G. Drentje, M. N. Harakeh, H. Sakai, and A. van der Woude, Phys. Lett. **130B**, 9 (1983).
 - [8] J. Arvieux, J. P. Albanese, M. Buenerd, and D. Lebrun, Phys. Rev. Lett. **42**, 753 (1979).
 - [9] T. D. Poelheken, S. K. B. Hesmondhalgh, H. J. Hofman, A. van der Woude, and M. N. Harakeh, Phys. Lett. B **278**, 423 (1992).
 - [10] H. Rost, W. Eyrich, A. Hofman, U. Scheib, F. Vogler, and H. Rebel, Phys. Lett. **88B**, 51 (1979).
 - [11] M. N. Harakeh and A. E. L. Dieperink, Phys. Rev. C **23**, 2329 (1981).
 - [12] S. Kamedzhiev, J. Speth, and G. Tertychny, Eur. Phys. J. A **7**, 483 (2000).
 - [13] Y.-W. Lui, H. L. Clark, and D. H. Youngblood, Phys. Rev. C **61**, 067307 (2000).